Original research

Novel subtype of mucopolysaccharidosis caused by arylsulfatase K (ARSK) deficiency

Sarah Verheyen,[1] Jasmin Blatterer,[1] Michael R Speicher,[1]
Gandham SriLakshmi Bhavani,[2] Geert-Jan Boons,[3,4] Mai-Britt Ilse,[5] Dominik Andrae,[5]
Jens Sproß,[6] Frédéric Maxime Vaz,[7] Susanne G Kircher,[8] Laura Posch-Pertl,[9]
Daniela Baumgartner,[10] Torben Lübke,[5] Hitesh Shah,[11] Ali Al Kaissi,[12]
Katta M Girisha ![ORCID],[2] Barbara Plecko ![ORCID] [13]

OPEN ACCESS

ABSTRACT

Background Mucopolysaccharidoses (MPS) are monogenic metabolic disorders that significantly affect the skeleton. Eleven enzyme defects in the lysosomal degradation of glycosaminoglycans (GAGs) have been assigned to the known MPS subtypes (I–IX). Arylsulfatase K (ARSK) is a recently characterised lysosomal hydrolase involved in GAG degradation that removes the 2-O-sulfate group from 2-sulfoglucuronate. Knockout of *Arsk* in mice was consistent with mild storage pathology, but no human phenotype has yet been described.

Methods In this study, we report four affected individuals of two unrelated consanguineous families with homozygous variants c.250C>T, p.(Arg84Cys) and c.560T>A, p.(Leu187Ter) in *ARSK*, respectively. Functional consequences of the two *ARSK* variants were assessed by mutation-specific *ARSK* constructs derived by site-directed mutagenesis, which were ectopically expressed in HT1080 cells. Urinary GAG excretion was analysed by dimethylene blue and electrophoresis, as well as liquid chromatography/mass spectrometry (LC-MS)/MS analysis.

Results The phenotypes of the affected individuals include MPS features, such as short stature, coarse facial features and dysostosis multiplex. Reverse phenotyping in two of the four individuals revealed additional cardiac and ophthalmological abnormalities. Mild elevation of dermatan sulfate was detected in the two subjects investigated by LC-MS/MS. Human HT1080 cells expressing the ARSK-Leu187Ter construct exhibited absent protein levels by western blot, and cells with the ARSK-Arg84Cys construct showed markedly reduced enzyme activity in an ARSK-specific enzymatic assay against 2-O-sulfoglucuronate-containing disaccharides as analysed by C18-reversed-phase chromatography followed by MS.

Conclusion Our work provides a detailed clinical and molecular characterisation of a novel subtype of mucopolysaccharidosis, which we suggest to designate subtype X.

INTRODUCTION

Glycosaminoglycans (GAGs) are essential components of the connective tissue. They consist of disaccharide units, each composed of a uronic acid (glucuronate or iduronate) and an N-acetyl-hexosamine (glucosamine or galactosamine), which are further modified by N-sulfation and O-sulfation. Mucopolysaccharidoses (MPS) result from enzymatic defects in the stepwise degradation of sulfated GAGs, leading to lysosomal storage of heparan sulfate (HS), chondroitin sulfate (CS), dermatan sulfate (DS), keratan sulfate (KS), or their degradation intermediates.[1] This typically results in multisystem disorders with variable manifestations including skeletal dysplasia (earlier termed 'dysostosis multiplex'), short trunk disproportionate short stature, coarse facial features, corneal and lens opacity, retinopathy, hypoacusis/hearing loss, valvular heart disease, cardiomyopathy, hepatosplenomegaly and, in some cases also neurodegeneration (OMIM: PS607014). Up to now, eleven different enzymes have been linked to MPS. Classification into different MPS subtypes was made clinically, depending on the phenotype and affected organ systems, followed by the assignment to specific enzyme defects. There is considerable overlap of the skeletal MPS phenotype with other disorders affecting the skeletal system, 461 of which have been summarised in the Nosology and Classification of Genetic Skeletal Disorders in 2019.[2] As elevated urinary GAG excretion is a diagnostic hallmark of MPS, total GAG analysis using dimethylmethylene blue (DMB) or uronic acid-based spectrophotometry and quantification of DS, HS and KS by liquid chromatography (LC) are commonly used methods for MPS screening in urine. Leucocyte enzyme activity assays and genetic testing can be used for specification and confirmation of respective MPS subtypes.[1 3]

Among other enzymes, several sulfatases are involved in the degradation of GAGs.[4] The human lysosomal arylsulfatase K (ARSK (OMIM:*610 011)) was identified by computational analysis of the human genome, based on its sulfatase-specific amino acid sequence at the catalytic site (sulfatase signature CXPSR).[5] As in all human sulfatases, the conserved cysteine within this sequence undergoes post-translational modification and is converted into an α-formylglycine residue, which is essential for the enzyme activity of all human sulfatases.[6] ARSK was found to remove the 2-O-sulfate group from 2-sulfoglucuronate, which led to its other designation 'glucuronate 2-sulfatase' (GDS). Glucuronate-2-O-sulfation occurs in HS, DS and CS and, during

degradation, is selectively removed by ARSK (online supplemental figure S1).[7] As sulfatases show no functional overlap and high substrate specificity,[8] ARSK deficiency was discussed as a possible cause of a yet unidentified MPS subtype.[9]

A recently published *Arsk*-deficient mouse model showed a mild lysosomal storage phenotype.[10] Glycan reductive isotope labelling-LC/mass spectrometry (MS) revealed HS and CS accumulation in various tissues. Otherwise, the mouse model was characterised by a slight but non-significant elevation of urinary GAG excretion in the absence of skeletal or neurological abnormalities, however, a mild behavioural phenotype was observed.[10]

Hence, although experimental data suggested an association of biallelic *Arsk*-variants with an MPS phenotype in mice, no association has yet been established in humans. This is the first report with a comprehensive phenotypical evaluation of four individuals from two unrelated families with ARSK (GDS) deficiency.

MATERIAL AND METHODS

Subjects and enrolment

In both families, parents were consanguineous and had two affected children with skeletal dysplasia, resembling spondyloepiphysial dysplasia. The first, female child of family 1 was designated as subject 1 (S1), the second, male child as subject 2 (S2). In family 2, the first two children were unaffected. The third and the fourth male children were indicated as subjects 3 (S3) and 4 (S4), respectively.

Family 1 was referred for genetic analysis from a specialised orthopaedic centre in Austria. Following the identification of *ARSK* as a candidate gene in family 1, a search for additional affected individuals was carried out using GeneMatcher,[11] which identified the second family in India.

Written informed consent for publication was obtained from both families. Explicit permission to publish photographs was obtained for S1 and S2.

Clinical investigations

Medical history and family history were taken during an onsite visit in all 4 subjects (S1–S4).

Reverse phenotyping was performed in subjects 1 and 2 after identifying the *ARSK* variant to search for further symptoms of MPS, including slit-lamp examination and funduscopy, audiometry, cardiac and abdominal ultrasound, neurological examination, and dermatological assessment. Subjects 3 and 4 have had a thorough assessment of their skeletal phenotype, but no complementary investigations were possible as the patients were not available for follow-up examinations.

Laboratory investigations

A peripheral blood smear was performed with Giemsa staining and was investigated using light microscopy.

GAG excretion in urine (24-hour collection and random sample) was analysed quantitatively with uronic acid and DMB in S1, respectively, and DMB in S2. High-resolution electrophoresis of urinary GAG excretion was performed using standard methods.[12 13]

Urine and plasma GAGs were measured using a multiplex assay with enzymatic digestion of HS, DS and KS followed by quantification of specific disaccharides by LC-MS/MS as described previously.[14]

Genetic analysis

In family 1 exome sequencing was performed in S1, using DNA from leucocytes in a diagnostic setting. DNA was extracted using the QIASymphony DSP DNA Midi Kit on a QIASymphony SP instrument (QIAGEN, Hilden, Germany). Nextera DNA Flex Library Prep Kit was used for library preparation and sequencing was performed on a NextSeq 550 (Illumina, San Diego, California, USA). Sequence alignment of raw fastq files to the human reference sequence (GRCh37/hg19 assembly) and variant calling was performed with the DRAGEN Germline Pipeline V.3.2.8 on Illumina BaseSpace (https://basespace.illumina.com/). Variant annotation, filtering and prioritisation using human phenotype ontology (HPO) terms (spondylometaphysial dysplasia HP:0002657 and disproportionate short-trunk short stature HP:0003521) was performed using VarSeq V.2.2 (Golden Helix, Bozeman, Montana, USA, www.goldenhelix.com). MPS-associated genes (*GALNS* [OMIM:*612 222], *GLB1* [OMIM:*611 458], *GNS* [OMIM:* 607 664], *GUSB* [OMIM:*611 499], *HYAL1* [OMIM:*607 071], *IDUA* [OMIM:*252 800], *ARSB* [OMIM:*611 542], *HGSNAT* [OMIM:*610 453], *NAGLU* [OMIM:*609 701], *SGSH* [OMIM:* 605 270], *IDS* [OMIM:*300 823]) were analysed separately in S1 to exclude a known MPS form. Sanger sequencing was performed for segregation analysis of the *ARSK* variant in S2 and the patients' parents.

In family 2 exome sequencing of the probands and two unaffected siblings was performed. Genomic DNA was extracted using the standard phenol-chloroform method. Exome was captured using Illumina's Nextera Rapid Capture Kit followed by massively parallel sequencing using the NextSeq500 Sequencer (Illumina, San Diego, California, USA) with a targeted average coverage depth of 100×. An inhouse pipeline with integrated burrows-wheeler aligner 1 and genome analysis toolkit V.3.6 best practices2 was used for data analysis. Variants were annotated using ANNOVAR3 and allele frequencies derived from 983 in-house exomes of Indian ethnicity, OMIM phenotypes and HPO terms were integrated in the annotation with the help of inhouse Perl scripts. Region of homozygosity (ROH) analysis was done with the help of FILTUS tool4 using exome data of affected and unaffected siblings. As the family has two affected siblings and reported consanguinity, a pathogenic variant was assumed in the shared homozygous region. The *ARSK* variant was validated by Sanger sequencing.

Generation of ARSK and ARSG constructs

Different *ARSK* constructs were generated to prove that the detected variant in family 1, NM_198150.2:c.250C>T, p.(Arg84Cys), results in reduced enzymatic function with a specific enzyme assay.

Wild type-*ARSK* (*ARSK*-WT) and *ARSK*-Cys80Ala constructs were used for comparison of enzymatic function, as normal function was defined by the WT-construct and loss of sulfatase activity had previously been shown for the Cys80Ala-construct.[9] An additional construct with the enzyme arylsulfatase G (*ARSG*[OMIM:* 610 008]), another human sulfatase, was used to show substrate specificity of ARSK.[15] All constructs used in this study include a C-terminal histidine-tag (RGSHHHHHH-tag).

The *ARSK*-Arg84Cys (c.250C>T) and *ARSK*-Leu187Ter (c.560T>A) constructs were derived by site-directed mutagenesis according to the QuickChange mutagenesis protocol (Agilent Technologies) using the following mutagenesis primers:
*ARSK*_c.250C>T_f:CAATTTGTTGCCCATCATGCGCAGCAATGTG
*ARSK*_c.250C>T_r:CACATTGCTGCGCATGATGGGCAACAAATTG

$ARSK\_c.560T>A\_f: GACAAAGCAGTAAACTGGT\underline{A}$
AAGAAAGGAAGC

$ARSK\_c.560T>A\_r: GCTTCCTTTCTTTACCAGTTTACT$
GCTTTGTC

The sequences of the resulting constructs were validated by Sanger sequencing.

Transfection and immunoblotting

ARSK-WT, *ARSK*-Arg84Cys, *ARSK*-Leu187Ter, *ARSK*-Cys80Ala and *ARSG* (N-sulfoglucosamine 3-O-sulfatase) were transiently expressed in HT1080 cells by polyethylenimine (PEI) transfection protocol. Cells were harvested 48 hours after transfection and lysed in phosphate-buffered saline (PBS)/0,5% TX100, sonication was performed on ice (3×10 s), and homogenates were obtained by centrifugation (15000 g, 4°C). Protein determination was performed by detergent compatible (DC) assay (BioRad). Homogenates (50 µg of total protein) were analysed by immunoblotting on polyvinylidene difluoride (PVDF) membrane and antibodies directed against ARSK (biorbyt 160024), ARSG (biorbyt 318995) and GAPDH (Santa Cruz sc-25778, FL-335) as loading control.

Western blot analysis

The effect of the loss-of-function variant, NM_198150.2:c.560T>A, p.(Leu187Ter), in family 2 was investigated by western blot analysis. We used cell lysates (50 µg of total protein) after PEI-mediated transient transfection of HT1080 cells with *ARSK*-WT, *ARSK*-Arg84Cys and *ARSK*-Leu187Ter, respectively.

Glucuronate-2-sulfatase activity assay

The disaccharide 2-sulfoglucuronate-N-acetyl-glucosamine (G2A0) was pre-labelled with the fluorescent dye 2-aminoacridone (AMAC).[10] AMAC-labelled G2A0 (12,5 nmol) was incubated with 100 µg protein of the appropriate homogenates in a final volume of 52,5 µl in 250 mM ammonium-acetate buffer pH 4.6 for 24 hours at 37°C. After centrifugation (15000 g, 4°C), the samples were analysed by C18-reversed-phase (RP)-chromatography in ammonium acetate buffer (60 mM, pH 5.6) with a flow rate of 1 mL/min with the Ettan LC system (GE Healthcare). The saccharides were eluted and fractionated with an acetonitrile gradient, in which AMAC-labelled disaccharides were detected by ultraviolet (UV) absorbance at 255 nm. The fractions containing AMAC-mediated fluorescence peaks were vacuum dried, resolved in 25 µl acetonitrile and analysed by nano-electrospray ionization mass spectrometry (ESI-MS) in a negative ion mode.

RESULTS

Biallelic *ARSK* variants cause a novel MPS phenotype

Genetic testing was performed in S1–S4 between the ages of 14 years and 20 years. Until then, their skeletal dysplasia has not been assigned to a specific genetic disorder. The main radiological abnormalities in all four subjects were thickened calvaria, platyspondyly, anterior inferior beaking of the thoracolumbar vertebrae, broadening of clavicles and ribs, narrowing of lower parts of iliac bones, small epiphyses, metaphysial striae, and hypoplastic carpal bones (online supplemental table S3, figures 1 and 2). Cranial MRI performed due to headache in S1 at 12 years of age showed normal results and absence of enlarged Virchow-Robin spaces.

Heart abnormalities in S1 and S2 included cardiac murmur (aortic or mitral), valve disease, thickened leaflets and
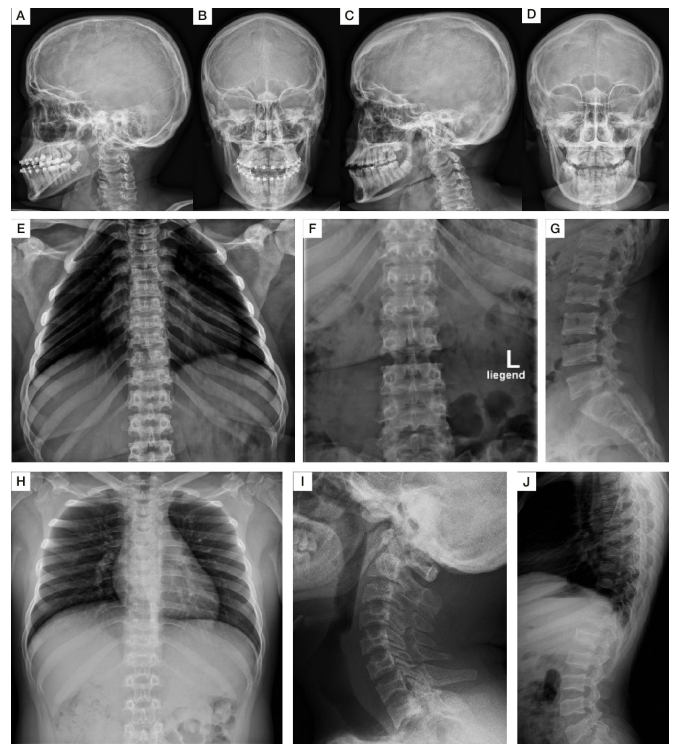
Figure 1 Phenotype of skull, thorax and spine. Lateral skull radiographs show mildly thickened calvarias of S1 (A, B) and S2 (C–D). S1 and S2 show an open bite (A, C). Radiographs of chest and spine show broad (oar-shaped) ribs (S1 at 17 years (E, F) and S2 at 14 years (H)), broad vertebral bodies, platyspondyly and irregular endplates (S1 at 17 years (G), S3 at 18 years (J)). S1 shows a bell-shaped thorax (E). Radiographs of lateral spine additionally illustrate anterior beaking and irregular vertebral end plates (J). Lateral spine radiograph of the lumbar area shows platyspondyly with scalloping of the posterior end plates (S1 at 12 years (G)). Anterior inferior beaking of the cervical spine of S3 at 20 years (I). S1–S4, subjects 1–4.

regurgitation. S1 also showed mild ventricular hypertrophy suggesting mild storage cardiomyopathy, a reduced distensibility of the aorta and an elevated stiffness, as additional known cardiac manifestations of MPS.

All four subjects of this study had normal behaviour and attended a regular school, S1 and S2 at A level. S3 and S4 were not available for follow-up examinations, therefore their behaviour and cognitive function in adulthood remains unknown.

Phenotypical features of S1 and S2 are shown in figure 3 and are summarised in table 1.

Reverse phenotyping in S1 and S2 clearly revealed an MPS phenotype with multisystem involvement. In these two subjects, coarse facial features, short trunk disproportionate short stature and short neck, genua valga, and hip pain were noticed at the end of the first decade. Furthermore, reverse phenotyping revealed mild opacity of the lens and vitreous body. The optical coherence tomography image of the retina of S1 showed loss of interdigitation zone temporal of the macula. Mild aortic valve stenosis and mild left ventricular hypertrophy were noted in cardiac ultrasound in S1 and S2.

Auditory tests revealed normal results in S1 and S2 at the age of 16 years and 14 years, respectively.

Early MPS-related symptoms like macrocephaly at birth (S1 and S2), recurrent ear infections (S2) and sleeping disorder (S2) were initially not attributed to an underlying genetic condition (see timeline figure 3J). Of note, head circumference in S3 and

Figure 2 Radiological abnormalities of the extremities. Hand radiographs demonstrate short third, fourth and fifth metacarpals, small carpal bones and small epiphyses of lower ends of radius and ulna (S2 at 14 years (A), S4 at 17 years (B), S3 at 18 years (C)). Posterior-Anterior (PA) projection hand radiograph of S2 at 14 years shows defective ossification of the carpal bones associated with retarded bone age. Apparent metaphysial irregularities and dysplasia along the metacarpophalangeal joints (A). PA right pelvis radiograph of S2 at 14 years (D) shows dysplasia and fragmentation of the capital femoral epiphysis associated with acetabular dysplasia. The shaft of the femur is overtubulated. Radiographs of the femora and tibiae demonstrate vertical striae in the metaphyses (S2 at 14 years (E), S4 at 17 years (F)). Tibia and fibula of S2 at 14 years show overtubulation of the shafts (G). Epi-metaphysial dysplasia of the inferior ends of the tibia and fibula. Metaphysial irregularities are associated with metaphysial striation (G). S1–S4, subjects 1–4.

S4 was below the third percentile, proportionate to height at the ages of 18 years and 17 years, respectively.

Absence of vacuolisation in peripheral leucocytes
A peripheral blood smear in S1 and S2 did not reveal abnormal vacuolisation in leucocytes.

Urinary GAG excretion pattern and plasma GAG concentration
Urine analysis in S1 at 11 years of age revealed normal urinary GAG excretion but elevated CS and KS excretion (online supplemental table S1).

These results led to the suspicion of MPS IVA (OMIM:#253000) or MPS IVB (OMIM:#253010) as in these MPS subtypes CS and KS typically show elevated values during childhood.[16] The thin-layer chromatography showed a normal pattern of oligosaccharides. Consecutive enzymatic analysis in blood showed normal activity of galactosamine-6-sulfatase and β-galactosidase, thus excluding MPS IVA and MPS IVB.

After identifying the homozygous *ARSK* variant, quantitative analysis of urinary GAGs with DMB and quantification of DS, HS, KS by high-resolution electrophoresis was repeated in S1 and S2 at the ages of 16 years and 14 years, respectively. The analysis revealed normal results in S1 and borderline total GAG excretion and slightly elevated CS in S2 (online supplemental table S1).
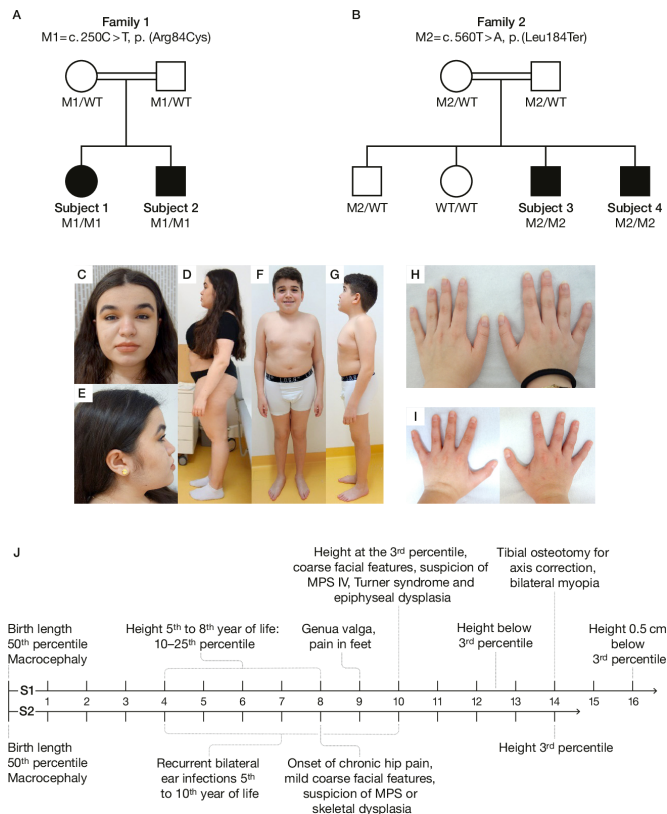
Figure 3 Overview of the subjects, their phenotype and health problems. Family 1: (A) pedigree, (C–E) S1 at the age of 16 years, (F, G) S2 at the age of 14 years. Family 2: (B) pedigree. S1–S2 show mild coarse facial features, midface retrusion, full lips (C, F), short-trunk short stature (D, F, G), (relative) macrocephaly (D, F, G), short neck (E, G) and genua valga (F). Hands are shaped normally (H, I). Onset of symptoms in S1 and S2 is depicted in the timeline, age in years (J). MPS, mucopolysaccharidoses; S1–S4, subjects 1–4; WT, wild type. M1=mutation in family 1; M2=mutation in family 2.

Measurement of urinary GAG excretion by LC-MS/MS analysis in S1 and S2 at the ages of 15 years and 17 years, respectively, showed a threefold and fourfold elevation of specific DS-derived disaccharides in a morning urine sample, respectively (online supplemental table S2), while all other specific GAG-derived disaccharides were in the normal range.

Measurement of plasma GAG concentrations by LC-MS/MS showed no clear difference in the disaccharide pattern of S1 and S2 when compared with 10 control samples, even when analysed in a subgroup of age-matched controls (online supplemental table S2).

Enzyme activity of ß-hexosaminidase, ß-galaktosidase, arylsulfatase A, α-iduronidase, iduronat-2-S sulfatase, sulfamidase, acetylglucosaminidase, GlcNAc-transferase, GlcNAc-6-S-sulfatase, GalNAc-6-S-sulfatase, arylsulfatase B and ß-glucuronidase was measured in fibroblasts of S2 and were all within normal range.

Identification of biallelic *ARSK* variants in four individuals with a skeletal disorder resembling spondyloepiphysial dysplasia
Exome analysis in S1 revealed a homozygous variant in *ARSK*, NM_198150.2:c.250C>T, p.(Arg84Cys), located within a 38.4 Mb sized ROH (GRCh37/hg19 Chr5:82940273–121330223). The variant was confirmed in a homozygous state in S2 and a heterozygous state in the patients' parents (figure 3A).

Table 1 Genetic variants and phenotype of patients with *ARSK* deficiency

	Subject 1 (family 1)	Subject 2 (family 1)	Subject 3 (family 2)	Subject 4 (family 2)
Variant in *ARSK* gene (NM_198150.2)	c.250C>T, p.(Arg84Cys), homozygous	c.250C>T, p.(Arg84Cys), homozygous	c.560T>A, p.(Leu187Ter), homozygous	c.560T>A, p.(Leu187Ter), homozygous
Ethnicity	Turkish	Turkish	Indian	Indian
Last examination (age in years, sex)	16 y, female	14 y, male	18 y, male	17 y, male
Previous suspected diagnoses	MPS, spondyloepiphysial dysplasia, Turner syndrome	MPS, spondyloepiphysial dysplasia	Brachyolmia, MPS, spondyloepiphysial dysplasia	Brachyolmia, MPS, spondyloepiphysial dysplasia
Height	146.5 cm, −3.25 SD	150 cm, −1.94 SD	157 cm, −3.22 SD	145.5 cm, −4.53 SD
Weight	68 kg	49 kg	n.a.	32.48 kg
Head circumference	59 cm, 2.52 SD	58.5 cm, 1.95 SD	53 cm, −2.21 SD	52.5 cm, −2.41 SD
Arm span	150.5 cm	155 cm	164 cm	147 cm
Length upper/lower body segment	71.5 cm / 75 cm	70 cm / 80 cm	73 cm / 84 cm	65.5 cm / 80 cm
Facial phenotype	Coarse facial features	Coarse facial features	Coarse facial features, long philtrum, broad nasal root	Coarse facial features, long philtrum, broad nasal root
Eyes	Mild myopia since 14th year of life, mild lens and vitreous opacity, mild retinal pigmentation temporal of the fovea	Mild lens and vitreous opacity, mild retinal pigmentation temporal of the fovea	Normal	Normal, no corneal opacity, normal fundus
Auditory system	Normal audiogram and tympanogram	Normal audiogram and tympanogram	Normal	Normal
Jaw and teeth	Open bite, wide spaced teeth, diastemata, canine-like appearance of lateral incisors	Open bite, wide spaced teeth, canine-like appearance of lateral incisors	Normal	Normal
Hands/wrist	Hands normal	Hands normal, intermittent paresthesia	Normal	Brachydactyly, arthropathy of right wrist
Skeletal features	Disproportionate short-trunk short stature, genu valgus, mild scoliosis	Disproportionate short-trunk short stature, mild genu valgus	Disproportionate short-trunk short stature, genu valgus	Disproportionate short-trunk short stature, genu valgus, mild scoliosis
Liver, spleen	Normal in size and structure (ultrasound examination)	Normal in size and structure (ultrasound examination)	Normal on clinical examination	Normal on clinical examination
Kidneys	Normal in size and structure (ultrasound examination)	Normal in size and structure (ultrasound examination)	n.a.	Operation for right renal calculus at 6 y
Heart	Systolic murmur, mild aortic valve stenosis and regurgitation, thickened ends of aortic cusps, mild left ventricular hypertrophy	Systolic and diastolic murmur, mild aortic valve stenosis and regurgitation, thickened ends of aortic cusps	Normal on clinical examination	Normal on clinical examination
Neurological examination, cognition	Normal	Normal	Normal	Normal

ARSK, arylsulfatase K; MPS, mucopolysaccharidosis; n.a., not available; y, years.

Targeted variant analysis of known MPS-associated genes in the exome data set of S1 did not reveal pathogenic or likely pathogenic variants in *GALNS*, *GLB1*, *GNS*, *GUSB*, *HYAL1*, *IDUA*, *ARSB*, *HGSNAT*, *NAGLU*, *SGSH* and *IDS*.

Exome analysis in family 2 revealed a homozygous nonsense-mutation in *ARSK*, NM_198150.2:c.560T>A, p.(Leu187Ter), in S3 and S4, located within a ROH of 14 Mb (GRCh37/hg19 Chr5:81721372–95865500). The parents and the unaffected brother were found to be heterozygotes. The unaffected sister did not carry this variant (figure 3B). Both variants have not been reported in variant databases such as ClinVar and Human Gene Mutation Database (HGMD). The detected missense variant c.250C>T, p.(Arg84Cys), results from a C to T substitution, replacing the highly conserved arginine at codon 250 with cysteine, an amino acid with highly different physicochemical properties. The variant affects the sulfatase signature (CXPSR) within the N-terminal sulfatase domain of the protein, which is essential for forming the catalytic site of sulfatases.[6] In gnomAD, this variant is listed with a total allele frequency of 0.002129%

(6/281810 alleles). The variant c.560T>A, p.(Leu187Ter), is listed with a total allele frequency of 0.0003980% (1/251248 alleles). Of note, no individuals with homozygous loss-of-function variants are represented in gnomAD.

Affected individuals' *ARSK* variants cause ARSK deficiency

The arginine at amino acid position 84 in ARSK is part of the highly conserved sulfatase signature 80-CCPSR-84 (online supplemental figure S2) and is crucial for efficient oxidation of the cysteine (Cys80) into a formylglycine residue. This post-translational modification is essential for enzyme activity of all human sulfatases.[6]

Ectopic expression of the constructs in HT1080 cell lysates revealed comparable expression levels for ARSK-WT, ARSK-Arg84Cys, slightly lower amounts of ARSK-Cys80Ala and lack of protein formation for *ARSK*-Leu187Ter in western blot analyses, using an ARSK-specific antibody (figure 4D, online supplemental figure S3D). This indicated comparable stability
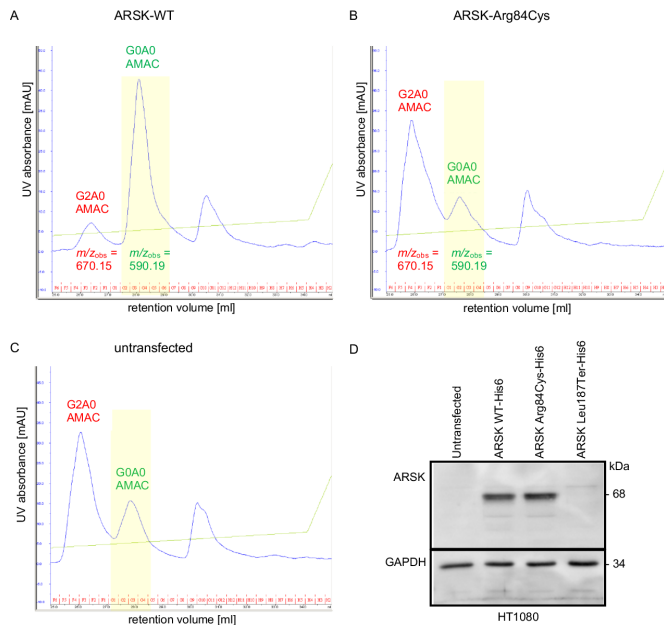
Figure 4 Investigation of the functional consequences of the *ARSK* variants. ARSK-WT but not ARSK-Arg84Cys desulfates synthetic 2-sulfoglucuronate-N-acetylglucosamine (G2A0) disaccharides (A, B). (A) G2A0 treated with cell lysates expressing ARSK-WT resulted in a minor peak at 26.5 mL representing the 2-O-sulfated educt (m/z 670.15) and a major peak at 28 mL retention volume representing the desulfated product (m/z 590.19), indicating the loss of a sulfate group (highlighted in yellow). Analysis with C18-reversed-phase chromatography. (B, C) Incubation of AMAC-labelled G2A0 disaccharide with ARSK-Arg84Cys cell lysates or with cell lysates of untransfected cells resulted in a main AMAC-peak at 26 mL (m/z 670.15). The G0A0-mediated fluorescence signal remained the minor peak in both samples. Of note, this minor peak in untransfected as well as in ARSK-Arg84Cys transfected cells results most likely from the activity of the endogenous ARSK of the HT1080 cells. The ubiquitous peak in the right of the chromatogram (>30 mL of retention volume) was not analysed in more detail as it was also present in unreacted samples. Western blot analysis (D): Comparable expression levels for ARSK-WT and ARSK-Arg84Cys but lack of ARSK-Leu187Ter in HT1080 cell lysates. This indicates comparable stability of ARSK-WT and ARSK-Arg84Cys and probable nonsense mediated mRNA-decay as a consequence of the Leu187Ter variant. Glyceraldehyde-3-phosphate dehydrogenase (GAPDH) was used as loading control. WT, wild type.

of ARSK-WT and ARSK-Arg84Cys, probable lower stability of ARSK-Cys80Ala, and was compatible with nonsense-mediated mRNA-decay or synthesis of a shortened and thereby highly instable polypeptide as a consequence of the Leu187Ter variant. ARSK-WT-HT1080, ARSK-Arg84Cys-HT1080 and ARSK-Cys80Ala-HT1080 cell lysates only revealed moderate differences in total acid sulfatase activity using the artificial pseudo-substrate p-nitrocatechol sulfate at acidic pH, indicating

Web resources

► ClinVar, https://www.ncbi.nlm.nih.gov/clinvar/
► GeneMatcher, https://genematcher.org/ gnomAD, http://gnomad.broadinstitute.org/
► HGMD, http://www.hgmd.cf.ac.uk/ac/index.php
► OMIM, http://www.omim.org

a high background of the entire set of endogenous lysosomal and non-lysosomal sulfatases (data not shown).

Therefore, we used the specific ARSK disaccharide substrate G2A0 prelabelled with the fluorescent dye AMAC at the reducing end of the N-acetylglucosamine residue, so that the non-reducing end of the disaccharide was still accessible for enzymatic degradation. After expressing the different ARSK constructs and the ARSG construct, respectively, HT1080 cell lysates were incubated with AMAC-labelled G2A0 and were subsequently analysed by RP HPLC fractionation. Incubation of the AMAC-labelled G2A0 substrate (26 mL retention volume, buffer control) with ARSK-WT homogenates resulted in a main AMAC-mediated detection peak with a retention volume of 28 mL indicating an efficient 2-O-desulfation of the disaccharide leading to the desulfated G0A0 product (figure 4A). However, most other samples (except the buffer sample) including the Cys80Ala variant and the ARSG (N-sulfoglucosamine 3-O-sulfatase) also showed a minor peak at 28 mL (online supplemental figure S3B,C), which was most likely due to endogenous ARSK activity in HT1080 cells rather than residual ARSK activity of ARSK-Arg84Cys and ARSK-Cys80Ala, respectively. MS analysis of indicated peak fractions (figure 4, online supplemental figure S3; m/z values) containing AMAC-labelled disaccharides revealed expected masses of m/z 670.15 for the 2-O-sulfated disaccharide educt peaks and m/z values of 590.19 for the desulfated product within the peaks shifted towards a higher retention volume (figure 4, online supplemental figure S3).

These data clearly demonstrate that the human ARSK-Arg84Cys variant, similar to the previously published ARSK-Cys80Ala construct, is not able to efficiently desulfate the glucuronate-2–0-sulfated disaccharide. Exchange of cysteine and arginine at positions 80 and 84, respectively, leads to strongly reduced sulfatase activity.

DISCUSSION

In this study, we report the identification of biallelic *ARSK* variants as the underlying cause of a novel subtype of MPS in four individuals of two unrelated families. Affected individuals had skeletal abnormalities and coarse facial features suggestive for MPS, while multisystem involvement with cardiac and ophthalmological findings was only identified by targeted reverse phenotyping.

We demonstrate that the *ARSK* variant c.250C>T, p.(Arg84Cys) in family 1 leads to ARSK deficiency, proven by a functional GDS assay, whereas the variant c.560T>A, p.(Leu187Ter) in family 2 results in the absence of any ARSK-specific signal in western blot analysis, most probably due to nonsense-mediated mRNA decay.

The effect of ARSK enzymatic deficiency on GAG storage in vivo was recently shown in an *Arsk* knockout mouse model.[10] 2-O-sulfated HS was increased in isolated liver lysosomes of *Arsk* KO mice,[10] while no evidence of storage pathology was noted in liver, spleen and kidney of S1–S2 by ultrasound examination. *Arsk*-deficient mice had a normal skeletal morphology, whereas skeletal abnormalities are the main feature in the human subjects of this study. Although the delineated phenotype in mice is milder and not directly comparable to the human phenotype assessed in this study, the mouse model provides additional evidence that ARSK deficiency leads to a novel subtype of MPS.[10]

Detailed history and reverse phenotyping of two of the affected individuals (S1 and S2) revealed recurrent bilateral ear infections and sleep disturbance, as noted in 80%–90% of children affected by MPS (type I, II, III, IV).[17] Assessment for

known ophthalmological features of MPS[18 19] revealed mild lens and vitreous opacity and mild pigmentary changes of the retina in S1 and S2. The heart abnormalities which were found in S1 and S2 are in accordance with those typically observed in MPS, like cardiac murmur (aortic or mitral), valve disease, ventricular hypertrophy, thickened leaflets, and regurgitation, reduced distensibility of the aorta and elevated stiffness.[20]

In S1 total urinary GAG excretion was normal at 11 years of age, which could be due to a decline of urinary GAG excretion with age.[21] Electrophoresis in S1 showed elevated excretion of CS and KS, pointing to a possible diagnosis of MPS IV, but enzyme analysis of galactosamine-6-sulfatase (Morquio A) and ß-galactosidase (Morquio B) was normal. Repeated GAG analysis in S1 and S2 at age 16 years and 14 years, respectively, revealed normal results. In addition, the application of the recently developed LC-MS/MS method for the analysis of specific GAG-derived disaccharides revealed a sensitivity for the DMB method of only 90%, underpinning the risk of false-negative results for MPS screening by DMB.[14] Urinary GAG analysis by LC-MS/MS in S1 and S2 at 17 years and 15 years of age, respectively, revealed a threefold and fourfold increase of specific DS-derived disaccharides. This is in line with the higher sensitivity of the LC-MS/MS method. The elevated proportion of CS (and KS) detected by electrophoresis in S1 at age 11 years and S2 at age 14 years, respectively, could probably be explained by the overlapping band of accumulated sulfated DS with CS and KS, while no unsulfated DS band was visible on either sample. We speculate that urinary GAG screening by DMB may fail to detect *ARSK*-associated MPS, which probably contributed to the late identification of this MPS type. Further studies with DMB and electrophoresis, as well as the detection of specific GAG-derived disaccharides by LC-MS/MS, are needed to characterise this novel MPS subtype at the level of accumulating compounds.

In conclusion, the results of this study establish a novel enzyme defect in the group of MPS. ARSK deficiency caused by biallelic loss-of-function mutations or missense mutations affecting the sulfatase signature is associated with childhood-onset disproportionate short-trunk short stature, and skeletal, cardiac and ophthalmological abnormalities. ARSK deficiency should be considered in patients with unclarified skeletal dysplasia or clinically suspected but unassigned MPS, even in the presence of normal urinary GAG excretion. We suggest designating ARSK deficiency as novel subtype X within the group of MPS.

Author affiliations
[1]Diagnostic and Research Center for Molecular BioMedicine, Medical University of Graz, Graz, Austria
[2]Department of Medical Genetics, Kasturba Medical College, Manipal, Manipal Academy of Higher Education, Manipal, India
[3]Complex Carbohydrate Research Center, University of Georgia, Athens, Georgia, USA
[4]Department of Chemistry, University of Georgia, Athens, Georgia, USA
[5]Department of Chemistry, Biochemistry, Bielefeld University, Bielefeld, Germany
[6]Faculty of Chemistry, Industrial Organic Chemistry and Biotechnology - Mass Spectrometry, Bielefeld University, Bielefeld, Germany
[7]Laboratory Genetic Metabolic Disease, Amsterdam UMC, University of Amsterdam, Departments of Clinical Chemistry and Pediatrics, Core Facility Metabolomics, Emma Children's Hospital, Amsterdam Gastroenterology Endocrinology Metabolism, Amsterdam, The Netherlands, Amsterdam UMC Locatie Meibergdreef, Amsterdam, North Holland, The Netherlands
[8]Institute of Medical Chemistry, Medical University of Vienna, Vienna, Austria
[9]Department of Ophthalmology, Medical University of Graz, Graz, Austria
[10]Department of Pediatrics and Adolescent Medicine; Division of Pediatric Cardiology, Medical University of Graz, Graz, Austria
[11]Department of Orthopedics, Kasturba Medical College Manipal, Manipal, India
[12]Pediatric Department, Speising Orthopaedic Hospital, Vienna, Austria
[13]Department of Pediatrics, Division of General Pediatrics, Medical University of Graz, Graz, Austria

ORCID iDs
Katta M Girisha http://orcid.org/0000-0002-0139-8239
Barbara Plecko http://orcid.org/0000-0002-3203-1325

REFERENCES
1 Lawrence R, Brown JR, Lorey F, Dickson PI, Crawford BE, Esko JD. Glycan-based biomarkers for mucopolysaccharidoses. *Mol Genet Metab* 2014;111:73–83.
2 Mortier GR, Cohn DH, Cormier-Daire V, Hall C, Krakow D, Mundlos S, Nishimura G, Robertson S, Sangiorgi L, Savarirayan R, Sillence D, Superti-Furga A, Unger S, Warman ML. Nosology and classification of genetic skeletal disorders: 2019 revision. *Am J Med Genet A* 2019;179:2393–419.
3 Kubaski F, de Oliveira Poswar F, Michelin-Tirelli K, Burin MG, Rojas-Málaga D, Brusius-Facchin AC, Leistner-Segal S, Giugliani R. Diagnosis of mucopolysaccharidoses. *Diagnostics* 2020;10:172.
4 Lübke T, Damme M. Lysosomal sulfatases: a growing family. *Biochem J* 2020;477:3963–83.
5 Obaya AJ. Molecular cloning and initial characterization of three novel human sulfatases. *Gene* 2006;372:110–7.
6 Dierks T, Lecca MR, Schlotterhose P, Schmidt B, von Figura K. Sequence determinants directing conversion of cysteine to formylglycine in eukaryotic sulfatases. *Embo J* 1999;18:2084–91.
7 Dhamale OP, Lawrence R, Wiegmann EM, Shah BA, Al-Mafraji K, Lamanna WC, Lübke T, Dierks T, Boons G-J, Esko JD. Arylsulfatase K is the lysosomal 2-Sulfoglucuronate sulfatase. *ACS Chem Biol* 2017;12:367–73.
8 Hanson SR, Best MD, Wong C-H. Sulfatases: structure, mechanism, biological activity, inhibition, and synthetic utility. *Angew Chem Int Ed Engl* 2004;43:5736–63.

9   Wiegmann EM, Westendorf E, Kalus I, Pringle TH, Lübke T, Dierks T, Dierks Arylsulfatase T T. Arylsulfatase K, a novel lysosomal sulfatase. *J Biol Chem* 2013;288:30019–28.

10   Trabszo C, Ramms B, Chopra P, Lüllmann-Rauch R, Stroobants S, Sproß J, Jeschke A, Schinke T, Boons G-J, Esko JD, Lübke T, Dierks T. Arylsulfatase K inactivation causes mucopolysaccharidosis due to deficient glucuronate Desulfation of heparan and chondroitin sulfate. *Biochem J* 2020;477:3433–51.

11   Sobreira N, Schiettecatte F, Valle D, Hamosh A. GeneMatcher: a matching tool for connecting Investigators with an interest in the same gene. *Hum Mutat* 2015;36:928–30.

12   Hopwood JJ, Harrison JR. High-resolution electrophoresis of urinary glycosaminoglycans: an improved screening test for the mucopolysaccharidoses. *Anal Biochem* 1982;119:120–7.

13   Whitley CB, Ridnour MD, Draper KA, Dutton CM, Neglia JP. Diagnostic test for mucopolysaccharidosis. I. Direct method for quantifying excessive urinary glycosaminoglycan excretion. *Clin Chem* 1989;35:374–9.

14   Langereis EJ, Wagemans T, Kulik W, Lefeber DJ, van Lenthe H, Oussoren E, van der Ploeg AT, Ruijter GJ, Wevers RA, Wijburg FA, van Vlies N. A multiplex assay for the diagnosis of mucopolysaccharidoses and mucolipidoses. *PLoS One* 2015;10:e0138622.

15   Kowalewski B, Lübke T, Kollmann K, Braulke T, Reinheckel T, Dierks T, Damme M. Molecular characterization of arylsulfatase G: expression, processing, glycosylation, transport, and activity. *J Biol Chem* 2014;289:27992–8005.

16   Blau N, Duran M, Gibson KM, Dionisi Vici C. *The Mucopolysaccharidoses. In: Physician's Guide to the Diagnosis, Treatment, and Follow-Up of Inherited Metabolic Diseases*. Springer, 2014: 449–64.

17   Galimberti C, Madeo A, Di Rocco M, Fiumara A. Mucopolysaccharidoses: early diagnostic signs in infants and children. *Ital J Pediatr* 2018;44:133.

18   Del Longo A, Piozzi E, Schweizer F. Ocular features in mucopolysaccharidosis: diagnosis and treatment. *Ital J Pediatr* 2018;44:125.

19   Ashworth JL, Biswas S, Wraith E, Lloyd IC. Mucopolysaccharidoses and the eye. *Surv Ophthalmol* 2006;51:1–17.

20   Boffi L, Russo P, Limongelli G. Early diagnosis and management of cardiac manifestations in mucopolysaccharidoses: a practical guide for paediatric and adult cardiologists. *Ital J Pediatr* 2018;44:122.

21   El Moustafa K, Sivri S, Karahan S, Coşkun T, Akbıyık F, Lay İncilay. Screening for mucopolysaccharidoses in the Turkish population: analytical and clinical performance of an age-range specific, dye-based, urinary glycosaminoglycan assay. *Clin Chim Acta* 2017;464:72–8.

Supplementary file

Novel subtype of mucopolysaccharidosis caused by arylsulfatase K (ARSK) deficiency

Sarah Verheyen, Jasmin Blatterer, Michael R. Speicher, Gandham SriLakshmi Bhavani, Geert-Jan Boons, Mai-Britt Ilse, Dominik Andrae, Jens Sproß, Frédéric M. Vaz, Susanne Gerit Kircher, Laura Posch-Pertl, Daniela Baumgartner, Torben Lübke, Hitesh Shah, Ali Al Kaissi, Katta M. Girisha,* Barbara Plecko*

Author information
Ali Al Kaissi, Katta M. Girisha and Barbara Plecko contributed equally as last authors.
Katta M. Girisha and Barbara Plecko share corresponding authorship.

*corresponding authors
barbara.plecko@medunigraz.at
Division of General Pediatrics, Department of Pediatrics and Adolescent Medicine, Medical University of Graz, 8036 Graz, Austria
girish.katta@manipal.edu
Department of Medical Genetics, Kasturba Medical College, Manipal, Manipal Academy of Higher Education, Manipal, India, 576104

Figure S1: The role of ARSK in heparan sulfate degradation as an example for GAG degradation

ARSK removes the 2-O-sulfate group from 2-sulfoglucuronate. This figure, showing GAG degradation with the example of heparan sulfate, is adapted with permission from Dhamale et al. (2017)[1], © 2017, American Chemical Society.

```
ARSA    SLCTPSRAALLTGRLPV    83
ARSB    PLCTPSRSQLLTGRYQI    105
ARSC    PLCTPSRAAFMTGRYPV    89
ARSD    PLCTPSRAAFLTGRHSF    103
ARSE    SLCTPSRAAFLTGRYPV    100
ARSF    SLCSPSRSAFLTGRYPI    93
ARSG    STCSPSRASLLTGRLGL    98
ARSH    SMCTPSRAAFLTGRYPI    69
ARSI    PICTPSRSQLLTGRYQI    107
ARSJ    PICTPSRSQFITGKYQI    136
GALNS   PLCSPSRAALLTGRLPI    93
GNS     ALCCPSRASILTGKYPH    105
SGSH    SSCSPSRASLLTGLPQR    84
SULF1   PMCCPSRSSMLTGKYVH    101
SULF2   PMCCPSRSSILTGKYVH    102
IDS     AVCAPSRVSFLTGRRPD    98
ARSK    PICCPSRAAMWSGLFTH    94
          *     *
```

Figure S2: Conserved sulfatase signature

The arginine in the CxPxR-motif is unexceptionally conserved in all human sulfatases indicating its relevance in formylglycine modification and catalytic activity.

Supplemental material

BMJ Publishing Group Limited (BMJ) disclaims all liability and responsibility arising from any reliance placed on this supplemental material which has been supplied by the author(s)

J Med Genet
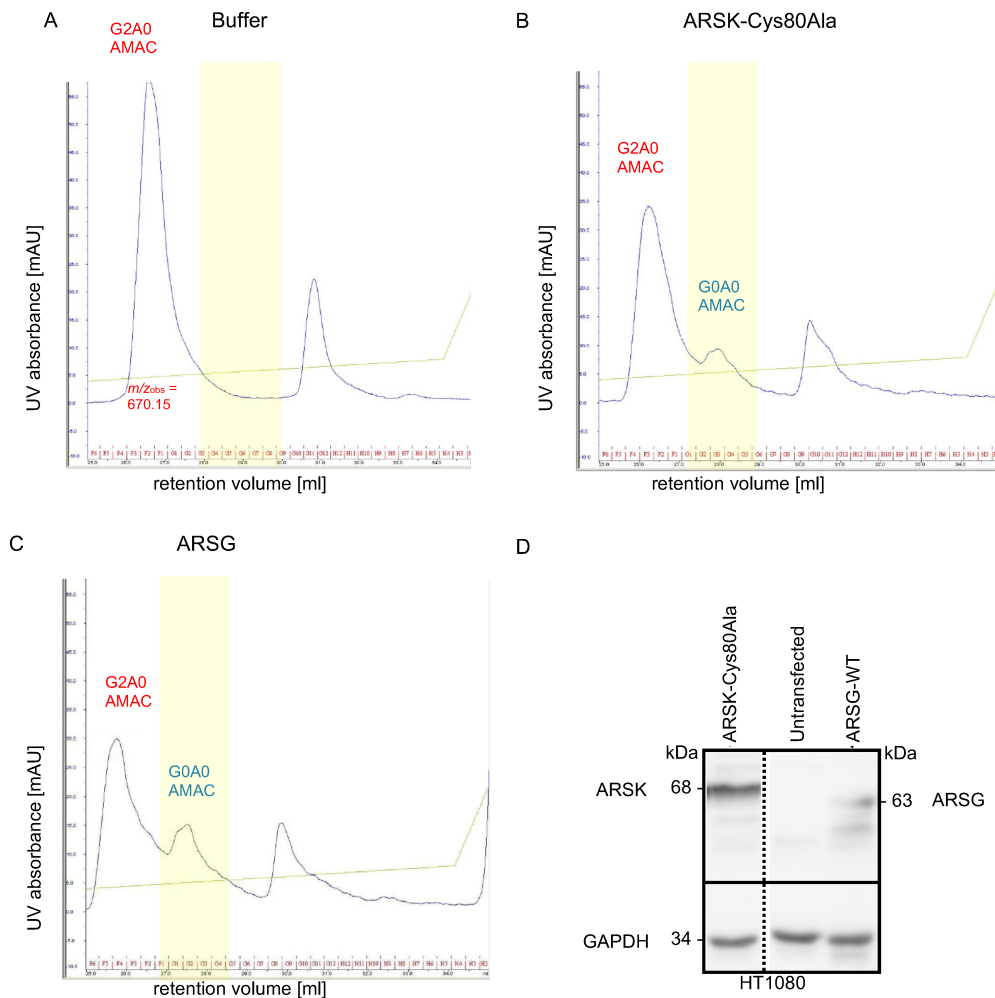
Figure S3: Functional consequences of ARSK variants - additional measurements

ARSK-Cys80Ala and ARSG did not desulfate the synthetic G2A0 disaccharides. Incubation of the AMAC-labeled G2A0 disaccharide with buffer only as control (a) resulted in a major peak of the unreacted educt (m/z 670.15) and ubiquitous peak at a retention volume > 30 ml). Incubation of AMAC-labeled G2A0 with ARSK-Cys80Ala (b) and ARSG (c) resulted in minor G0A0 product peaks, which might be attributed to the activity of endogenous HT1080 ARSK rather than to ectopic expression of ARSK-Cys80Ala or ARSG, respectively. (d) Western blot analysis: Expression of ARSK-Cys80Ala in HT1080 cell lysates. No expression in untransfected or ARSG-transfected cells. GAPDH was used as loading control.

Supplemental material

BMJ Publishing Group Limited (BMJ) disclaims all liability and responsibility arising from any reliance
placed on this supplemental material which has been supplied by the author(s)

J Med Genet

Figure S4: Progression of skeletal dysplasia – hands of S1-4 at different ages

Hand radiographs of affected individuals demonstrate short third, fourth and fifth metacarpals, small carpal bones and small epiphyses of lower ends of radius and ulna. S1 at 10 years (A) and 12 years (B), S2 at 14 years (C), S4 at 17 years (D), S3 at 18 years (E)
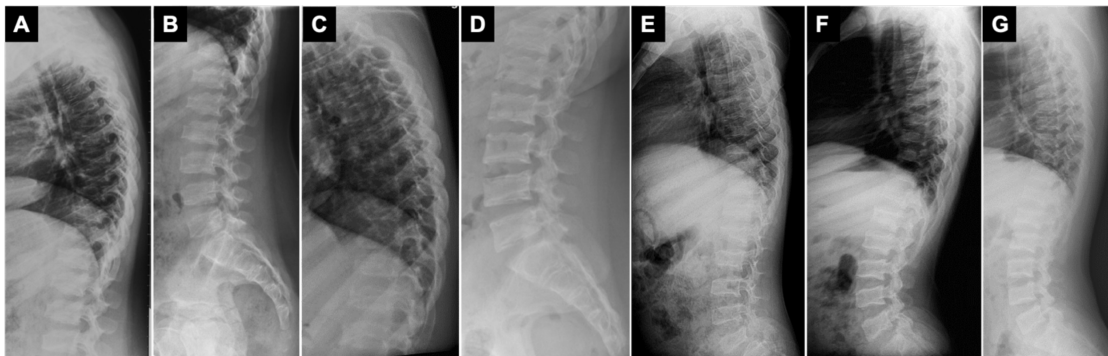
Figure S5: Progression of skeletal dysplasia – lateral spine of S1-4 at different ages

Radiographs of lateral spine illustrate platyspondyly, anterior beaking and irregular vertebral end plates. S1 at 12 years (A, B), S2 at 14 years (C), S1 at 17 years (D), S4 at 17 years (E), S3 at 18 years (F) and at 20 years (G)

Figure S6: Progression of skeletal dysplasia – pelvis of S1-4 at different ages

Pelvic radiographs of affected individuals demonstrate irregular acetabular roofs, reduced hip joint space and small capital femoral epiphyses. S1 at 12 years (A), S2 at 14 years (B), S4 at 17 years (C), S3 at 18 years (D) and at 20 years (E)

5

Supplemental material

BMJ Publishing Group Limited (BMJ) disclaims all liability and responsibility arising from any reliance placed on this supplemental material which has been supplied by the author(s)

J Med Genet

Table S1: Results of DMB urine electrophoresis in S1 (age 11 and 16 years) and S2 (age 14 years)

	DMB urine analysis		
	S1 (at 11 years)*¹	**S1 (at 16 years)*²**	**S2 (at 14 years)*²**
GAG mg /creatinine mmol (DMB method)	8.9 mg/mmol	7 mg/mmol	18 mg/mmol
	expected <18 mg/mmol	expected ≤10 mg/mmol	expected ≤18 mg/mmol
Chondroitin sulfate	67%	78%	**93% ↑**
	expected 70-80%	expected 70-80%	expected 70-80%
Heparan sulfate	9%	22%	7%
	expected 20-30%	expected 20-30%	expected 20-30%
Keratan sulfate	**24%**	not detected	not detected
	expected undetectable	expected undetectable	expected undetectable

*1: analyses performed at the Center of Pathobiochemistry and Genetics, Medical University of Vienna, Austria
*2: analysis performed at the Laboratory of Metabolic Diseases, Department of Pediatrics and Adolescent Medicine, Medical University of Graz, Austria

Table S2: Results of LC-MS/MS analysis of urine and plasma in S1 (age 17 years) and S2 (age 15 years)

	LC-MS/MS urine analysis*³		LC-MS/MS plasma analysis*³	
	S1 (at 17 years)	**S2 (at 15 years)**	**S1 (at 17 years)**	**S2 (at 15 years)**
Dermatan sulfate	**165 µg/mmol creatinine ↑**	**234 µg/mmol creatinine ↑**	42 ng/ml	39 ng/ml
	expected 0-53 µg/mmol creatinine		average in reference samples: 34 ng/ml, range 8 - 131 ng/ml	
Heparan sulfate	230 µg/mmol creatinine	288 µg/mmol creatinine	131 ng/ml	146 ng/ml
	expected 0-323 µg/mmol creatinine		average in reference samples: 257.2 ng/ml, range 66 - 1346 ng/ml	
Keratan sulfate	60 µg/mmol creatinine	239 µg/mmol creatinine	839 ng/ml	2146 ng/ml
	expected 0-314 µg/mmol creatinine		average in reference samples: 1017.1 ng/ml, range 457 - 2442 ng/ml	
Total GAG content in plasma			1012 ng/ml	2330 ng/ml
			average in reference samples 1308.3 ng/ml, range 619 - 2691 ng/ml	

*3: analysis performed at the Laboratory Genetic Metabolic Diseases, Amsterdam UMC, University of Amsterdam, Departments of Clinical Chemistry and Pediatrics, Core Facility Metabolomics, Emma Children's Hospital, Amsterdam Gastroenterology Endocrinology Metabolism, Amsterdam, The Netherlands

6

Table S3: ARSK-associated skeletal phenotype

ARSK-associated skeletal phenotype in comparison to radiologic MPS-specific features						
Radiologic MPS specific features[2-6]		**S1**	**S2**	**S3**	**S4**	**Subject specific details**
Skull	Thickened cortical bone of the calvaria	x	x	x	x	
Spine	Rounded or bullet-shape vertebral bodies	-	-	-	-	Irregular vertebral end plates
	Platyspondyly	x	x	x	x	
	Anterior inferior beaking of the thoracolumbar vertebrae	x	x	x	x	
	Posterior scalloping of the vertebral bodies.	x	x	x	x	
	Thoracolumbar junction kyphosis	-	-	-	-	
	Kyphosis with gibbus	-	-	-	-	
	Hyperlordosis	-	-	x	x	
	Scoliosis	-	x	-	x	
	Spinal cord compression	-	-	-	-	
Hip/pelvis	Poor development of acetabulum and medial proportion of proximal femoral epiphysis	x	x	x	x	Irregular acetabular roofs, reduced hip joint space
	Severe hip dysplasia	x	x	x	x	
Hands/feet	Carpal and tarsal bones are hypoplastic and irregularly shaped	x	x	x	x	
	Metacarpal bones are proximally pointed, shortened and thickened	x	x	x	x	Short third, fourth and fifth metacarpals
Long bones	Hypoplastic and thinned epiphyses cortically with osteoporosis	x	x	x	x	Small epiphyses of lower ends of radius, ulna and capital femur
		x	x	x	x	Metaphyseal striae
Chest/ribs	Abnormally shaped ribs, spatulate ribs, broadening of clavicles and ribs	x	x	x	x	

7

References

1   Dhamale OP, Lawrence R, Wiegmann EM, Shah BA, Al-Mafraji K, Lamanna WC, Lubke T, Dierks T, Boons GJ, Esko JD. Arylsulfatase K is the Lysosomal 2-Sulfoglucuronate Sulfatase. *ACS Chem Biol* 2017;12(2):367-373.

2   Oussoren E, Wagenmakers EM, Link B, van der Meijden JC, Pijnappel W, Ruijter GJG, Langeveld M, van der Ploeg AT. Hip disease in Mucopolysaccharidoses and Mucolipidoses: A review of mechanisms, interventions and future perspectives. *Bone* 2021;143:115729.

3   Nicolas-Jilwan M, AlSayed M. Mucopolysaccharidoses: overview of neuroimaging manifestations. *Pediatr Radiol* 2018;48(10):1503-1520.

4   Spina V, Barbuti D, Gaeta A, Palmucci S, Soscia E, Grimaldi M, Leone A, Manara R, Polonara G. The role of imaging in the skeletal involvement of mucopolysaccharidoses. *Ital J Pediatr* 2018;44(Suppl 2):118.

5   Melbouci M, Mason RW, Suzuki Y, Fukao T, Orii T, Tomatsu S. Growth impairment in mucopolysaccharidoses. *Mol Genet Metab* 2018;124(1):1-10.

6   White KK. Orthopaedic aspects of mucopolysaccharidoses. *Rheumatology (Oxford)* 2011;50 Suppl 5:v26-33.